

Synthesis, docking and ADME prediction of novel 1,2,3-triazole-tethered coumarin derivatives as potential neuroprotective agents

Maddineni Aruna Kumari¹ · Chunduri Venkata Rao¹  ·
Settypalli Triloknadh¹ · Nallapaneni Harikrishna¹ ·
Chintha Venkataramaiah² · Wudayagiri Rajendra² ·
Daggupati Trinath² · Yeguvapalli Suneetha²

Received: 22 June 2017 / Accepted: 17 November 2017
© Springer Science+Business Media B.V., part of Springer Nature 2017

Abstract In an attempt to find potential neuroprotective agents, a series of novel 3-(1-((1-(substituted phenyl)-1*H*-1,2,3-triazol-4-yl) methoxyimino) ethyl)-2*H*-chromen-2-one derivatives **6a–j** were synthesized by using “click reaction” and evaluated for their *in vitro* neuroprotectivity and toxicity against H₂O₂-induced PC12 cell lines by using MTT (3-[4,5-dimethylthiazol-2-yl]-2,5-diphenyltetrazolium bromide) reduction assay. Most of them exhibited moderate to good activity in which compound **6e** was found to have significant protectivity with cell viability of 94.51 ± 0.68% at 50 µg/ml concentration and half-maximal effective concentration (EC₅₀) value of 14.04 µg/ml against injured PC12 cell lines and low toxicity with half-maximal cytotoxic concentration (CC₅₀) value of 544.88 µg/ml. Furthermore, molecular docking was carried out in order to understand plausible binding modes of novel derivatives with the active site of glycogen synthase kinase-3β enzyme, and the results were well complemented by the *in vitro* neuroprotective results against H₂O₂-induced PC12 cell lines. Additionally, *in silico* ADME properties showed drug likeness with good oral absorption and moderate blood–brain barrier permeability. The structures of all the synthesized compounds were confirmed by ¹H NMR, ¹³C NMR, IR and LC–MS analyses.

Keywords Click reaction · PC12 cell lines · Neuroprotective activity · Molecular docking · ADME prediction

✉ Chunduri Venkata Rao
cvrsvu@gmail.com

¹ Department of Chemistry, Sri Venkateswara University, Tirupati, Andhra Pradesh 517 502, India

² Department of Zoology, Sri Venkateswara University, Tirupati, Andhra Pradesh 517 502, India

Introduction

Neuroprotection is one of the major challenges of modern medicine for the treatment of neurodegenerative disorders, such as Parkinson's, Alzheimer's and Huntington's diseases [1]. Increased oxidative stress has been recognized as the main cause of many neurological disorders [2, 3]. Oxidative stress is often the result of unregulated production of reactive oxygen species including hydrogen peroxide, nitric oxide, super oxide and reactive hydroxyl radicals. Compared with other organs in the body, the central nervous system is mainly susceptible to oxidative stress because it is rich in highly oxygen-consuming polyunsaturated fatty acids and possesses a relatively low level of anti-oxidants and low regenerative capacity. Thus, the synthesis and development of neuroprotective agents has become an increasingly important area of research in recent years.

Both natural and synthetic coumarins (2*H*-1-benzopyran-2-ones) are attractive oxygen-containing fused heterocycles used in drugs, dyes, perfumes, cosmetics, optical brighteners, and fluorescent and laser dyes. Coumarins are plant flavonoids widely distributed in nature. The potent antibiotics like novobiocin, coumermycin and chlorobiocin are natural coumarin derivatives. The synthetic coumarin derivatives also have a wide range of biological activities against bacteria [4], fungi [5], tumors [6], viruses [7] and HIV protease [8]. They also act as anticoagulants [9], free radical scavengers [10], and lipoxygenase [11] and cyclooxygenase [12] inhibitors. In addition, coumarin derivatives exhibit good cell permeability. Furthermore, the activity of coumarin depends on the position and nature of the substituents present on it.

Click chemistry is a modular approach to generate 1,2,3-triazoles in a reliable and quantitative manner. In particular, Huisgen [3 + 2] cycloaddition between terminal alkynes and an azide in the presence of a Cu(I) catalyst generates 1,4-disubstituted 1,2,3-triazoles. They are characterized by biological activities like antiproliferative activity [13], antimicrobial [14], antidiabetic [15], anti-inflammatory [16], anticonvulsant [17], antineoplastic [18], antimalarial [19], and antiviral agents [20].

Coumarin derivatives, like 4-hydroxycoumarin, scopoletin, coumarin-3-carboxylic acid, fraxetin, 3,8-dimethyl-5-isopropyl-6-methoxycoumarin, etc., are naturally occurring cytotoxic coumarins. Recently, it has been reported that the nitrogen heterocycle at the 3-position of coumarin might contribute to neuroprotective activity. Several 3-substituted coumarin derivatives have been synthesized and proved to possess neuroprotective activity. Sun et al. [21] synthesized several substituted piperazinyl-linked coumarin scaffolds and examined their *in vitro* neuroprotective activity against OGD-induced PC12 cell lines (Fig. 1, I, II).

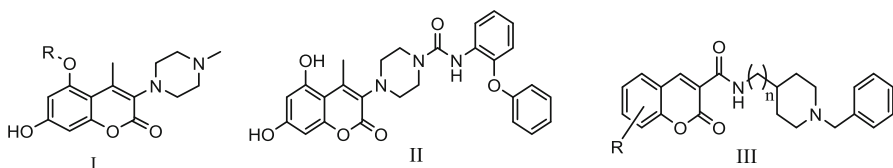


Fig. 1 Previously synthesized 3-substituted coumarin derivatives possessing neuroprotective activity

Asadipour et al. [22] synthesized novel coumarin-3-carboxamides bearing *N*-benzyl piperidine moiety and determined their inhibitory activity against AChE and BuChE and also protectivity against H₂O₂ induced PC12 cell lines (Fig. 1, III). Based on the above cited observations, we have recognized the importance of Fig. 1, nitrogen heterocycle at the 3rd position of coumarin to develop neuroprotective agents, and here we have reported the regioselective synthesis of novel 1,2,3-triazole derivatives **6a–j** through oxime functionality at the 3rd position of coumarin and their in vitro evaluation of neuroprotective activity against H₂O₂-induced PC12 cell lines using conventional MTT assay. PC12 cells were selected due to their similarity with dopaminergic neurons. Further, there is significant evidence that GSK-3 β , a member of the protein kinase family, plays a crucial role in neuro-degeneration [23]. Not only that, but GSK-3 β is abundantly found in the central nervous system and granulovascular degenerated neurons [24]. Accordingly, we opted to dock our synthesized molecules at the ATP binding pocket of the GSK-3 β enzyme. In addition, we have also used an in silico method to predict ADME properties in order to suggest the suitability of any of the new compounds for further drug development.

Materials and methods

Chemistry

Melting points were determined in open capillaries on a Mel Temp apparatus and are uncorrected. All the reactions were monitored by thin layer chromatography (TLC) on precoated silica gel 60 F254 (mesh); spots were visualized with UV light. Merck silica gel (60–120 mesh) was used for column chromatography. The IR spectra were recorded on a Perkin Elmer BX1 FTIR Spectrophotometer as KBr pellets and the wave numbers are given in cm⁻¹. ¹H NMR (400 MHz), and ¹³C NMR (100 MHz) spectra were recorded on a Bruker AMX 400 MHz NMR spectrometer in CDCl₃ solution using TMS as an internal standard. All chemical shifts are reported in δ (ppm) using TMS as an internal standard. The mass spectra were recorded on an Agilent 1100 LC/MSD instrument with method API-ES at 70 eV. Elemental analysis was determined using a Vario Microcube Elemental Analyzer.

General procedure for the synthesis of 3-acetyl-2H-chromen-2-one (2)

The mixture of salicylaldehyde **1** (1 mmol, 8.6 g) and ethyl aceto acetate (1 mmol, 9 ml) was stirred under cooling conditions. To this, a few drops of piperidine were added and stirring continued a yellow solid mass was obtained which was recrystallized from ethanol to get the pure compound **2**. Yield: 95%, m.p: 110 °C; IR (KBr, ν cm⁻¹): 1690 (C=O), 1717.5 (ester C=O), 3040 (aromatic CH); ¹H NMR (400 MHz, CDCl₃) δ _H: 2.72 (s, 3H, CH₃), 7.33–7.38 (m, 2H, Ar-H), 7.64–7.68 (m, 2H, Ar-H), 8.50 (s, 1H); ¹³C-NMR (100 MHz, CDCl₃) δ : 30.1, 116.2, 117.8, 124.1,

124.5, 129.8, 133.9, 147.0, 154.8, 158.7, 195.0; LC–MS (positive ion mode): m/z 211 $[M + Na]^+$ for $C_{11}H_8O_3$.

General procedure for the synthesis of 3-(1-(hydroxyimino)ethyl)-2H-chromen-2-one (3)

To a solution of compound **2** (1 mmol, 0.5 g) in dichloromethane, hydroxyl amine hydrochloride (4 mmol, 0.7 g) followed by sodium acetate (6 mmol, 0.9 g) were added and stirred at room temperature for 8 h. Then, the mixture was poured into crushed ice and extracted with dichloromethane. The extracted organic layer was distilled to get a solid product. It was purified by column chromatography using hexane and ethyl acetate mixture (30%) as an eluent. Yield: 90%, m.p: 170 °C; IR (KBr, ν cm^{-1}): 1597.9 (C=N), 1704.9 (C=O), 2890 (CH), 3043.4 (aromatic CH), 3227.1 (O–H); 1H NMR (400 MHz, $CDCl_3$) δ_H : 2.28 (s, 3H), 7.26–7.35 (m, 2H), 7.55 (d, $J = 6.7$ Hz, 2H), 7.92 (s, 1H), 11.21 (s, 1H, O–H); ^{13}C -NMR (100 MHz, $CDCl_3$) δ : 15.3, 117.3, 119.6, 125.4, 125.5, 129.4, 133.0, 142.3, 154.8, 156.0, 160.3; LC–MS (positive ion mode): m/z 204 $[M + 1]^+$ for $C_{11}H_9NO_3$.

General procedure for the synthesis of 3-(1-(prop-2-ynoxyimino) ethyl)-2H-chromen-2-one (4)

To a solution of compound **3** (1 mmol, 0.3 g) in acetone, potassium carbonate (3 mmol, 0.7 g) was added. To this, propargyl bromide (1.5 mmol, 0.2 ml) was added under inert atmosphere (N_2 gas) and stirring continued at room temperature overnight. After completion of the reaction, the mixture was poured into crushed ice. The separated precipitate was filtered and dried. This solid was purified by column chromatography using 15% hexane and ethyl acetate mixture as a mobile phase. Yield: 85%, m.p: 130 °C; IR (KBr, ν cm^{-1}): 1605.9 (C=N), 1712.2 (C=O), 2115.7 (C \equiv C), 3264.1 (\equiv CH); 1H NMR (400 MHz, $CDCl_3$) δ_H : 2.27 (s, 3H, CH_3), 2.51 (s, 1H, acetylene CH), 4.79 (s, 2H, CH_2), 7.27–7.35 (m, 3H, Ar–H), 7.55 (d, $J = 6.7$ Hz, 1H, Ar–H), 7.93 (s, 1H, Ar–H); ^{13}C -NMR (100 MHz, $CDCl_3$) δ : 14.5, 61.8, 74.7, 79.6, 116.5, 118.8, 124.6, 124.8, 128.6, 132.2, 141.5, 154.1, 155.2, 159.6; LC–MS (positive ion mode): m/z 242 $[M + H]^+$, 264 $[M + Na]^+$ for $C_{14}H_{11}NO_3$.

General procedure for the synthesis of aryl azides (5)

Aniline derivative (9.1 mmol) was dissolved in concentrated HCl (91 mmol) at room temperature and cooled to 0 °C, followed by the addition of an aqueous solution of sodium nitrite (45.5 mmol). The reaction mixture was stirred for 30 min at 0–5 °C. Then, an aqueous solution of sodium azide (27.3 mmol) was added and the mixture was further stirred for 2 h at room temperature. After completion of the reaction, the mixture was extracted with hexane. The combined organic layer was dried over anhydrous sodium sulfate. After evaporation of the solvent the desired azide derivative was obtained.

General procedure for the synthesis of 3-(1-((1-(substituted phenyl)-1H-1,2,3-triazol-5-yl)methoxyimino)ethyl)-2H-chromen-2-one (6a-j)

To a solution of compound **4** (0.7 mmol) in 2 ml of THF:H₂O (1:1) solvent mixture, CuSO₄·5H₂O (0.17 g, 0.7 mmol) was added and the reaction mixture was stirred for 5 min. To this light blue colour mixture sodium ascorbate (0.2 g, 1.05 mmol) was added and stirred for 15 min. The reaction mixture colour becomes dark yellow. After that aryl azide **6** (1.05 mmol) was added and allowed to stir at room temperature for 30 min-1 h. After that the reaction mixture was partitioned between ethyl acetate and water. The combined organic layer was dried over anhydrous sodium sulfate. The solvent was distilled and the crude product was purified by silica gel column chromatography using hexane ethyl acetate mixture as an eluent.

3-(1-((1-p-tolyl)-1H-1,2,3-triazol-4-yl)methoxyimino)ethyl)-2H-chromen-2-one (6a)
Yield: 70%, m.p: 120 °C; IR (KBr, ν cm⁻¹): 1609.9 (C=N), 1722.7 (C=O), 2856.2 (CH₂), 2921.2 (=CH); ¹H NMR (400 MHz, CDCl₃) δ _H: 2.27 (s, 3H), 2.42 (s, 3H), 5.43 (s, 2H), 7.28–7.35 (m, 4H), 7.55 (d, *J* = 7.5 Hz, 2H), 7.63 (d, *J* = 8.2 Hz, 2H), 7.9 (s, 1H), 8.05 (s, 1H, triazole CH); ¹³C-NMR (100 MHz, CDCl₃) δ : 14.8, 21.3, 68.0, 116.7, 119.0, 120.7, 121.5, 124.5, 124.8, 125.1, 128.7, 130.4, 132.4, 135.0, 139.1, 141.6, 154.2, 154.6, 159.7; LC-MS (positive ion mode): *m/z* 375 [M + H]⁺, 397 [M + Na]⁺ for C₂₁H₁₈N₄O₃. Anal. calcd. for C₂₁H₁₈N₄O₃: C, 67.37; H, 4.85; N, 14.96; found: C, 67.68; H, 4.73; N, 14.69.

3-(1-((1-(3-fluorophenyl)-1H-1,2,3-triazol-4-yl)methoxyimino)ethyl)-2H-chromen-2-one (6b) Yield: 75%, m.p: 125 °C; IR (KBr, ν cm⁻¹): 1126.8 (C-F), 1603.6 (C=N), 1701.6 (C=O), 2893.5 (CH₂), 3071.4 (=CH); ¹H NMR (400 MHz, CDCl₃) δ _H: 2.27 (s, 3H, CH₃), 5.43 (s, 2H, CH₂), 7.29–7.36 (m, 3H), 7.50 (d, *J* = 5.8 Hz, 1H), 7.54 (s, 1H), 7.56–7.59 (m, 3H), 7.89 (s, 1H), 8.12 (s, 1H, triazole CH); ¹³C-NMR (100 MHz, CDCl₃) δ : 14.3, 67.3, 116.3, 118.5, 118.7, 120.9, 123.0, 123.4, 124.4, 124.6, 128.2, 130.7, 131.5, 132.0, 137.6, 141.1, 145.3, 153.7, 154.2, 159.2; LC-MS (positive ion mode): *m/z* 379 [M + H]⁺, 401 [M + Na]⁺ for C₂₀H₁₅FN₄O₃. Anal. calcd. For C₂₀H₁₅FN₄O₃: C, 63.49; H, 4.00; N, 14.81; found: C, 63.88; H, 4.23; N, 14.59.

3-(1-((1-(4-methoxyphenyl)-1H-1,2,3-triazol-4-yl)methoxyimino)ethyl)-2H-chromen-2-one (6c) Yield: 80%, m.p: 130 °C; IR (KBr, ν cm⁻¹): 1252.2 (C–O–C), 1606.5 (C=N), 1718.2 (C=O), 2911.6 (CH₂), 3070.8 (=CH); ¹H NMR (400 MHz, CDCl₃) δ _H: 2.26 (s, 3H, CH₃), 3.87 (s, 3H, OCH₃), 5.42 (s, 2H, CH₂), 7.02 (d, *J* = 8.8 Hz, 2H), 7.27–7.35 (m, 3H), 7.54 (d, *J* = 7.3 Hz, 1H), 7.66 (d, *J* = 8.8 Hz, 2H, Ar-H), 7.9 (s, 1H), 8.02 (s, 1H, triazole CH); ¹³C-NMR (100 MHz, CDCl₃) δ : 14.5, 51.5, 67.8, 116.5, 118.8, 120.5, 121.2, 121.3, 123.4, 124.3, 124.6, 124.9, 128.5, 130.2, 132.2, 138.9, 154.0, 154.4, 159.5; LC-MS (positive ion mode): *m/z* 391 [M + H]⁺, 413 [M + Na]⁺ for C₂₁H₁₈N₄O₄. Anal. calcd. For C₂₁H₁₈N₄O₄: C, 64.61; H, 4.65; N, 14.35; found: C, 64.88; H, 4.73; N, 14.09.

3-(1-((1-(3-(trifluoromethyl)phenyl)-1H-1,2,3-triazol-4-yl)methoxyimino)ethyl)-2H-chromen-2-one (6d) Yield: 60%, m.p: 140 °C; IR (KBr, ν cm⁻¹): 1111.7 (C-F),

1608.9 (C=N), 1703.3 (C=O), 2888.9 (CH₂), 3075 (=CH); ¹H NMR (400 MHz, CDCl₃) δ_H: 2.27 (s, 3H, CH₃), 5.44 (s, 2H, CH₂), 7.29–7.36 (m, 3H), 7.69–7.72 (m, 3H), 7.89 (s, 1H), 7.99 (d, *J* = 7.6 Hz, 1H), 8.08 (s, 1H), 8.19 (s, 1H, triazole CH); ¹³C-NMR (100 MHz, CDCl₃) δ: 14.7, 67.4, 116.3, 117.3, 118.5, 119.6, 121.0, 123.3, 124.4, 128.2, 130.2, 131.2, 132.0, 134.3, 141.1, 143.2, 143.5, 144.3, 154.9, 156.4, 159.9; LC-MS (positive ion mode): *m/z* 429 [M + H]⁺, 451 [M + Na]⁺ for C₂₁H₁₅F₃N₄O₃. Anal. calcd. For C₂₁H₁₅F₃N₄O₃: C, 58.88; H, 3.53; N, 13.08; found: C, 59.08; H, 3.73; N, 13.23.

3-(1-((1-(3-nitrophenyl)-1*H*-1,2,3-triazol-4-yl)methoxyimino)ethyl)-2*H*-chromen-2-one (**6e**) Yield: 65%, m.p: 135 °C; IR (KBr, ν cm⁻¹): 1528.5 (NO₂), 1605.3 (C=N), 1706.6 (C=O), 2855.7 (CH₂), 2920.0 (=CH); ¹H NMR (400 MHz, CDCl₃) δ_H: 2.27 (s, 3H, CH₃), 5.45 (s, 2H, CH₂), 7.52–7.58 (m, 4H, Ar-H), 7.76 (s, 1H), 7.9 (s, 1H), 8.28–8.32 (m, 3H, Ar-H), 8.66 (s, 1H, triazole CH); ¹³C-NMR (100 MHz, CDCl₃) δ: 13.5, 66.6, 115.5, 117.8, 118.0, 120.2, 122.2, 122.6, 123.6, 123.8, 127.5, 130.0, 130.7, 131.2, 136.9, 140.4, 144.6, 152.9, 153.5, 158.5; LC-MS (positive ion mode): *m/z* 406 [M + H]⁺, 428 [M + Na]⁺ for C₂₀H₁₅N₅O₅. Anal. calcd. For C₂₀H₁₅N₅O₅: C, 59.26; H, 3.73; N, 17.28; found: C, 59.38; H, 3.78; N, 17.35.

3-(1-((1-(2-fluorophenyl)-1*H*-1,2,3-triazol-4-yl)methoxyimino)ethyl)-2*H*-chromen-2-one (**6f**) Yield: 60%, m.p:128 °C; IR (KBr, ν cm⁻¹): 1162.6 (C-F), 1602.8 (C=N), 1701.8 (C=O), 2933.1 (CH₂), 3060.0 (=CH); ¹H NMR (400 MHz, CDCl₃) δ_H: 2.19 (s, 3H, CH₃), 5.36 (s, 2H, CH₂), 7.19–7.27 (m, 3H), 7.43–7.48 (m, 5H), 7.82 (s, 1H), 8.03 (s, 1H, triazole CH); ¹³C-NMR (100 MHz, CDCl₃) δ: 12.7, 64.8, 114.6, 115.0, 115.9, 117.7, 118.7, 123.1, 123.7, 124.4, 126.7, 127.7, 130.0, 131.2, 133.0, 134.3, 141.1, 147.8, 152.7, 159.0; LC-MS (positive ion mode): *m/z* 401 [M + Na]⁺ for C₂₀H₁₅FN₄O₃. Anal. calcd. For C₂₀H₁₅FN₄O₃: C, 63.49; H, 4.00; N, 14.81; found: C, 63.88; H, 4.23; N, 14.96.

3-(1-((1-(*p*-phenyl)-1*H*-1,2,3-triazol-4-yl)methoxyimino)ethyl)-2*H*-chromen-2-one (**6g**) Yield: 75%, m.p: 110 °C; IR (KBr, ν cm⁻¹): 1600.8 (C=N), 1716.3 (C=O), 2856.7 (CH₂), 2919.5 (=CH), 3051.8 (Aromatic C-H); ¹H NMR (400 MHz, CDCl₃) δ_H: 2.27 (s, 3H, CH₃), 5.44 (s, 2H, CH₂), 7.27–7.35 (m, 3H), 7.44 (d, *J* = 7.5 Hz, 1H), 7.51–7.56 (m, 5H), 7.9 (s, 1H), 8.11 (s, 1H, triazole CH); ¹³C-NMR (100 MHz, CDCl₃) δ: 14.2, 67.5, 112.9, 115.6, 117.1, 120.1, 121.6, 122.8, 128.4, 129.2, 129.8, 131.3, 131.9, 134.3, 142.7, 143.2, 149.0, 157.2; LC-MS (positive ion mode): *m/z* 361 [M + H]⁺, 383 [M + Na]⁺ for C₂₀H₁₆N₄O₃. Anal. calcd. For C₂₀H₁₆N₄O₃: C, 66.66; H, 4.48; N, 15.55; found: C, 66.89; H, 4.73; N, 15.39.

3-(1-((1-(4-chlorophenyl)-1*H*-1,2,3-triazol-4-yl)methoxyimino)ethyl)-2*H*-chromen-2-one (**6h**) Yield: 60%, m.p: 120 °C; IR (KBr, ν cm⁻¹): 1605.4 (C=N), 1702.9 (C=O), 2888.9 (CH₂), 3070.1 (=C-H); ¹H NMR (400 MHz, CDCl₃) δ_H: 2.2 (s, 3H), 5.35 (s, 2H), 7.21–7.28 (m, 4H), 7.47 (d, *J* = 7.47 Hz, 2H), 7.56 (d, *J* = 8.24 Hz, 2H), 7.83 (s, 1H), 7.98 (s, 1H, triazole CH); ¹³C-NMR (100 MHz, CDCl₃) δ: 13.5, 66.7, 115.5, 117.8, 119.5, 120.2, 122.4, 123.3, 123.6, 123.9, 127.5, 129.2, 131.2, 133.7, 137.8, 140.3, 152.9, 158.5; LC-MS (positive ion mode): *m/z* 395 [M + H]⁺,

397 [M + 3H]⁺, 417 [M + Na]⁺ for C₂₀H₁₅ClN₄O₃. Anal. calcd. For C₂₀H₁₅ClN₄O₃: C, 66.84; H, 3.83; N, 14.19; found: C, 66.88; H, 4.03; N, 14.09.

3-(1-((1-(4-bromophenyl)-1H-1,2,3-triazol-4-yl)methoxyimino)ethyl)-2H-chromen-2-one (**6i**) Yield: 50%, m.p: 130 °C; IR (KBr, ν cm⁻¹): 1598.7 (C=N), 1704 (C=O), 2894.2 (CH₂), 3068.2 (=CH); ¹H NMR (400 MHz, CDCl₃) δ _H: 2.26 (s, 3H, CH₃), 5.44 (s, 2H, CH₂), 7.08 (d, *J* = 7.2 Hz, 2H), 7.13 (d, *J* = 7.5 Hz, 2H), 7.52–7.56 (m, 4H), 7.88 (s, 1H), 8.1 (s, 1H, triazole CH); ¹³C-NMR (100 MHz, CDCl₃) δ : 13.7, 67.7, 115.5, 116.5, 119.7, 120.2, 121.5, 123.3, 123.6, 123.4, 125.5, 130.2, 131.2, 138.8, 140.3, 152.9, 153.4, 159.5; LC-MS (positive ion mode): *m/z* 439 [M + H]⁺, 441 [M + 3H]⁺, 461 [M + Na]⁺ for C₂₀H₁₅BrN₄O₃. Anal. calcd. For C₂₀H₁₅BrN₄O₃: C, 54.69; H, 3.44; N, 12.75; found: C, 54.88; H, 3.73; N, 12.59.

3-(1-((1-(3-bromophenyl)-1H-1,2,3-triazol-4-yl)methoxyimino)ethyl)-2H-chromen-2-one (**6j**) Yield: 55%, m.p: 135 °C; IR (KBr, ν cm⁻¹): 1592.9 (C=N), 1704.8 (C=O), 2891.8 (CH₂), 3066.2 (=CH); ¹H NMR (400 MHz, CDCl₃) δ _H: 2.27 (s, 3H, CH₃), 5.43 (s, 2H, CH₂), 7.29–7.36 (m, 3H), 7.42 (d, *J* = 8.1 Hz, 1H), 7.54–7.58 (m, 3H), 7.89 (s, 1H), 7.98 (s, 1H), 8.1 (s, 1H, triazole CH); ¹³C-NMR (100 MHz, CDCl₃) δ _C: 14.5, 67.6, 116.5, 118.8, 119.0, 121.2, 123.3, 123.7, 124.7, 128.5, 130.2, 131.0, 131.7, 132.3, 137.9, 141.4, 145.6, 154.0, 154.5, 159.5; LC-MS (positive ion mode): *m/z* 439 [M + H]⁺, 441 [M + 3H]⁺, 461 [M + Na]⁺ for C₂₀H₁₅BrN₄O₃. Anal. calcd. For C₂₀H₁₅BrN₄O₃: C, 54.69; H, 3.44; N, 12.75; found: C, 54.88; H, 3.73; N, 12.59.

Biological activity

In vitro cytotoxic and neuroprotective activity

Cell lines The PC12 cell lines were purchased from the National Center for Cell Sciences, Pune. The cells were maintained in Dulbecco's Modified Eagle Medium (DMEM) supplemented with 8% horse serum, 2% FBS, 100 μ g/ml penicillin and 100 μ g/ml streptomycin in a water-saturated atmosphere of 5% CO₂ at 37 °C. The medium was changed every 3 days, and the confluent cells were passaged weekly by trypsinization.

MTT assay A forty-eight-hour monolayer culture of PC12 cells at a concentration of one lakh/well was seeded in 24-well titer plates. To the washed cell sheet with MEM without FCS, 1 ml of medium (without FCS) was added containing defined concentrations of the drug in respective wells. The stock drug was prepared by adding 10 mg of drug to 10 ml of serum-free MEM to give a concentration of 1 mg/ml. Working stock was prepared by mixing 4.5 ml of MEM and 0.5 ml of stock to give 1 mg/ml. To the cell control wells, 1 ml MEM (w/o) FCS was added and incubated at 37 °C in 5% CO₂ environment. After incubation, 200 μ l of MTT at a concentration of 5 mg/ml was added to each well and incubated for 6–7 h in 5% CO₂ atmosphere. After incubation, 1 ml of DMSO was added to each well and left for 45 s. Then, the quantity of metabolized MTT product dissolved in DMSO was

measured by determining the absorbance at 595 nm on a microplate reader by taking DMSO as a blank.

$$\text{Cell viability (\%)} = \text{Mean OD/Control OD} \times 100$$

Docking studies Molecular docking was used to estimate the binding free energy and binding mode of the synthesized compounds **6a–j** with GSK-3 β . Molecular docking was performed with PyRx 0.8 implementation of Auto Dock 4.2 [25] using an empirical free energy force field and Lamarckian genetic algorithm conformational search with the default parameters. The grid box was set around the ATP pocket in GSK3 β with a 45 Å \times 42 Å \times 46 Å grid box having 0.375-Å grid point spacing.

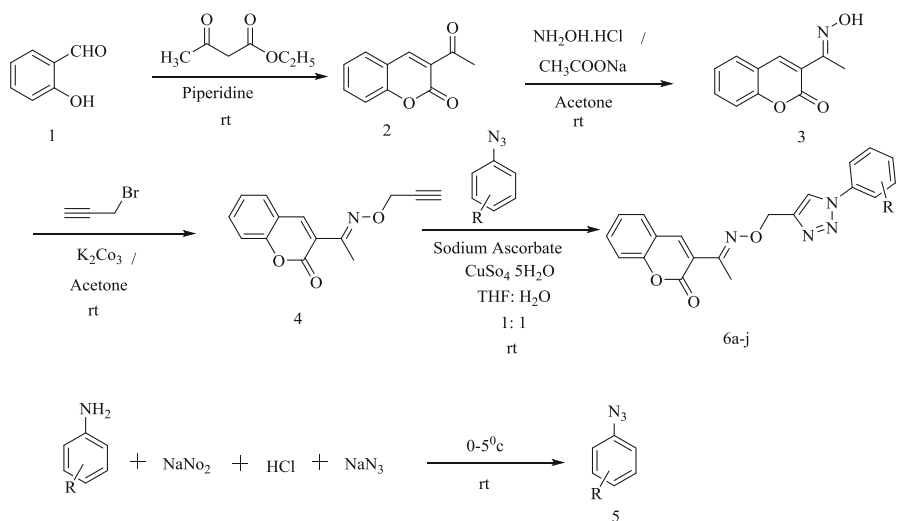
Target structure and ligand dataset preparation The 3D coordinates of the crystal structure GSK-3 β bounded with a native ligand, AR-A014418, in the ATP pocket was selected from the RCSB Protein Data Bank (PDB code: 1Q5 K) as the receptor model. The ATP pocket is present at the interface of β -strand domain (residues 25–138) at the N-terminal end and the α -helical domain (residues 139–343) is bordered by a glycine-rich loop and hinge region [26]. Water molecules and hetero atoms were removed from the co-crystal structure. Hydrogen atoms and Gasteiger partial charges were added to the target protein using UCSF Chimera 1.10.2 [27]. The compounds were subjected to energy minimization using the Open Babel module in PyRx program.

In silico ADME prediction The synthesized compounds were subjected to prediction of ADME properties. The various ADME properties including topological polar surface area (TPSA), molecular weight, number of rotatable bonds, molecular volume, number of hydrogen bond donors, number of hydrogen bond acceptors, mi Log *P* and violations of Lipinski rule were calculated by the Molinspiration online property toolkit. %ABS was calculated by using the formula: %ABS = 109 – (0.345 \times TPSA) [28]. ADME prediction properties like HIA%, CaCO₂ permeability, PPB%, and blood–brain barrier (BBB) were predicted by using pre-ADMET online server (<http://preadmet.bmdrc.org/>).

Results and discussion

Chemistry

The synthesis of 1,2,3-triazole-coumarin hybrids is outlined in Scheme 1. The target molecules synthesis consists of three parts. It involves the preparation of 3-(1-(hydroxyimino) ethyl)-2*H*-chromen-2-one (**3**) by treating 3-acetyl coumarin with hydroxylamine hydrochloride in sodium acetate and then treatment with propargyl bromide under nitrogen atmosphere in the presence of potassium carbonate to form 3-(1-(prop-2-ynyloxyimino) ethyl)-2*H*-chromen-2-one (**4**) and it is further converted into 3-(1-(((1-(substitutedphenyl)-1*H*-1,2,3-triazol-5-yl)methoxyimino)ethyl)-



Scheme 1 Schematic representation for the synthesis of 3-((1-(4-methoxyphenyl)-1H-1,2,3-triazol-5-yl)methoxyimino)ethyl)-2H-chromen-2-one (**6a–j**). Where R = 4-CH₃: **6a**, **5a**; R = 2-F: **6f**, **5f**; R = 3-F: **6b**, **5b**; R = H: **6g**, **5g**; R = 4-OCH₃: **6c**, **5c**; R = 4-Cl: **6h**, **5h**; R = 3-CF₃: **6d**, **5d**; R = 4-Br: **6i**, **5i**; R = 3-NO₂: **6e**, **5e**; R = 3-Br: **6j**, **5j**

2H-chromen-2-one derivatives **6a–j** by reacting with different aryl azides **5a–j** through click reaction. Initially, the 3-acetyl coumarin (**2**) was synthesized by Knoevenagel condensation between salicylaldehyde and ethyl acetoacetate in the presence of piperidine as a catalyst.

All the synthesized compounds were characterized by ¹H NMR, ¹³C NMR, IR and LC–MS spectra and elemental analysis. The formation of compound **2** was confirmed by the appearance of peaks at 1717.54 and 1705.12 cm⁻¹ due to C=O stretching in the IR spectra. Apart from this, a signal at δ 195.02 ppm in ¹³C NMR due to ester carbonyl carbon indicated the formation of coumarin. The peaks at 3227.06 and 1597.88 cm⁻¹ due to OH and C=N stretching, respectively, confirmed the formation of oxime derivative **3**. In addition to this, a signal at δ 11.21 ppm due to OH proton in ¹H NMR spectra also confirmed the formation of oxime. Further, the formation of propargyl derivative **4** was confirmed by the appearance of a peak at 3264.07 cm⁻¹ in its IR spectra due to ≡CH stretching and also by a singlet at δ 2.51 ppm in ¹H NMR spectra due to acetylenic CH proton. In the ¹H NMR spectra, the formation of triazole ring was confirmed by the resonance of H–C (**5**) of the triazole ring in the aromatic region, i.e. from δ 7.98 to 8.66 ppm.

Biology

In vitro neuroprotective activity

With all the target compounds in hand, neuroprotective activity was assayed against oxidative stress-induced PC12 cells by using MTT assay. H₂O₂ was used as toxic

insult to introduce oxidative damage. H_2O_2 can generate exogenous free radicals, which are highly reactive species which lead to lipid, protein and DNA damage. PC12 cells are usually used for studying neurodegenerative diseases [29, 30]. In this assay, the addition of $30\ \mu M$ H_2O_2 to growth medium significantly reduced cell viability to 48% compared to control. PC12 cells were incubated with coumarin analogs at concentrations ranging from 10 to $50\ \mu g/ml$ for 6–7 h, which was followed by the incubation with $30\ \mu M$ of H_2O_2 for 24 h. The protective effect of coumarin analogs against H_2O_2 was determined by the cell viability through MTT assay. MTT is named (3-(4,5-dimethyl thiazol-2yl)-2,5-diphenyl tetrazolium bromide. MTT is reduced by succinate dehydrogenase system of mitochondrial living cells to produce purple formazan crystals [31, 32]. After solubilization, the formazan can be measured spectrophotometrically and the amount of formazan produced is directly proportional to the number of viable cells in the culture (Table 1).

The cell viability values are shown in Table 2 and the results indicated that the cell viability rates significantly increase in a concentration-dependent manner from 10 to $50\ \mu g/ml$. Compounds **6a**, **6d** and **6f** also showed neuroprotectivity even at $10\ \mu g/ml$ concentration, but the remaining compounds lacked protectivity against H_2O_2 -induced PC12 cell lines at this concentration due to toxicity. Compounds **6h**, **6i** and **6j** did not show any neuroprotectivity even at $30\ \mu g/ml$ concentration. When the concentration reached $40\ \mu g/ml$, all compounds started to exhibit protectivity. Highest cell viability was observed for compounds **6e**, **6a**, **6b**, **6d** and **6f** at $50\ \mu g/ml$ concentrations of the test compounds. The graphical representation of these values is shown in Fig. 2.

The EC_{50} values of the compounds **6a–j** are in the range of 13.21 to $46.68\ \mu g/ml$ as shown in Fig. 3. Of all the compounds, **6a**, **6e** and **6f**, possessing *para* methyl phenyl, *meta* nitro phenyl and *ortho* fluoro phenyl, respectively, showed excellent protectivity with EC_{50} values 13.21, 14.04 and $15.66\ \mu g/ml$, respectively. The protectivity of compounds **6b**, **6c** and **6d** was moderate. The remaining compounds, **6g**, **6h**, **6i** and **6j**, exhibited very poor neuroprotectivity.

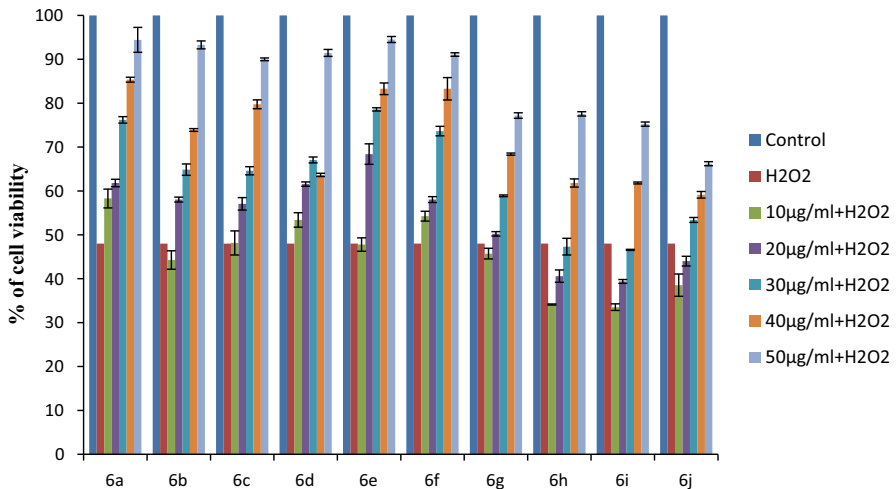
The structure activity relationship of compounds **6a–j** demonstrated that substitution of the electron-withdrawing nitro group at the *meta* position of the phenyl ring increased the protectivity of compound **6e** against damaged PC12 cell lines in the concentration range of $20–50\ \mu g/ml$. Moreover, it is worth noting that the presence of the electron-releasing methyl group at the *para* position improved the activity of compound **6a** compared with that of compound **6e**. This is possibly due to the lower toxicity of compound **6a** compared with that of compound **6e**. Compound **6a** exhibited protection in the range of $10–50\ \mu g/ml$ concentrations. Looking at the halogen derivatives, the type and position of the halogen atom in the phenyl ring have a variable influence on the activity. As the size of the halogen atom increases, the activity decreased gradually due to steric hindrance. This was observed in compounds **6h** and **6i**. The cell viability of compound **6h** which is a *para* chloro-substituted derivative is more than that of compound **6i** which is a *para* bromo substituted derivative in the concentration range $10–50\ \mu g/ml$. Similarly, for compound **6b** (a *meta* fluoro derivative) protectivity is more than that of **6j** (a *meta* bromo derivative) from 10 to $50\ \mu g/ml$ concentrations. Furthermore, the presence of

Table 1 Cell viability of compounds **6a-j** on H₂O₂-induced PC12 cells

Compound	% of cell viability						
	Control	H ₂ O ₂	10 µg/ml + H ₂ O ₂	20 µg/ml + H ₂ O ₂	30 µg/ml + H ₂ O ₂	40 µg/ml + H ₂ O ₂	50 µg/ml + H ₂ O ₂
6a	100	48	58.29 ± 2.15	61.82 ± 0.85	76.21 ± 0.74	85.36 ± 0.56	94.43 ± 2.83
6b	100	48	44.26 ± 2.1	58.04 ± 0.56	64.87 ± 1.29	73.90 ± 0.31	93.29 ± 0.89
6c	100	48	48.17 ± 2.74	57.07 ± 1.41	64.60 ± 0.92	79.75 ± 1.02	90.00 ± 0.32
6d	100	48	53.41 ± 1.65	61.58 ± 0.49	67.07 ± 0.67	73.65 ± 0.37	91.46 ± 0.79
6e	100	48	47.80 ± 1.53	68.41 ± 2.34	78.59 ± 0.37	83.29 ± 1.32	94.51 ± 0.68
6f	100	48	54.26 ± 1.13	58.04 ± 0.67	73.65 ± 1.09	83.29 ± 2.56	91.08 ± 0.39
6g	100	48	45.73 ± 1.22	50.24 ± 0.51	58.90 ± 0.18	68.41 ± 0.25	77.19 ± 0.63
6h	100	48	34.14 ± 0.12	40.60 ± 1.4	47.31 ± 1.89	61.82 ± 0.92	77.56 ± 0.49
6i	100	48	33.53 ± 0.74	39.39 ± 0.43	46.58 ± 0.13	61.82 ± 0.22	75.24 ± 0.48
6j	100	48	38.53 ± 2.54	44.02 ± 1.11	53.41 ± 0.56	59.14 ± 0.75	66.21 ± 0.46

Table 2 Results obtained from molecular docking studies of compounds **6a–j**

Compound	ΔG_b (kcal/mol) ^a	K_i (μM) ^b	H–B ^c	aa H–B ^d	H–B length ^e (\AA)
6a	– 7.51	3.13	3	Y134 (3)	2.6, 2.7, 3.1
6b	– 6.86	9.34	3	Y134 (2), R141 (1)	2.7, 3.3, 3.3
6c	– 6.54	16.06	0	–	–
6d	– 6.21	28.05	3	Y134 (2), R141 (1)	2.9, 3.1, 3.4
6e	– 8.3	0.82	4	Y134, V135, R141, R144	2.7, 3.3, 2.7, 3.0
6f	– 6.99	7.53	2	R141 (2)	3.1, 3.3
6g	– 6.69	12.39	1	R141	3.5
6h	– 6.43	19.48	1	Y134	2.9
6i	– 6.97	7.75	0	–	–
6j	– 6.59	14.79	2	Y134 (2)	3.2

^aBinding energy^bInhibition constant^cNumber of hydrogen bonds^dAmino acids involving hydrogen bonds^eHydrogen bond length between amino acids and compounds **6a–j****Fig. 2** Protective effects of compounds **6a–j** on H_2O_2 -induced cell death in PC12 cells. Cells were incubated with different concentrations (10–50 $\mu\text{g}/\text{ml}$) of compounds **6a–j** for 6 h and then treated with 30 μM H_2O_2 for 24 h. Cell viability was measured by MTT assay. Data are shown as mean \pm SD of three independent experiments

a fluorine atom at the *ortho* position improves the protectivity of compound **6f** compared with that of the *meta* fluorine-substituted derivative **6b** in the range of 10–40 $\mu\text{g}/\text{ml}$ concentrations. Moreover, compound **6f** showed protectivity even from 10 $\mu\text{g}/\text{ml}$ concentrations, but for compound **6b** protection starts from 20 $\mu\text{g}/\text{ml}$

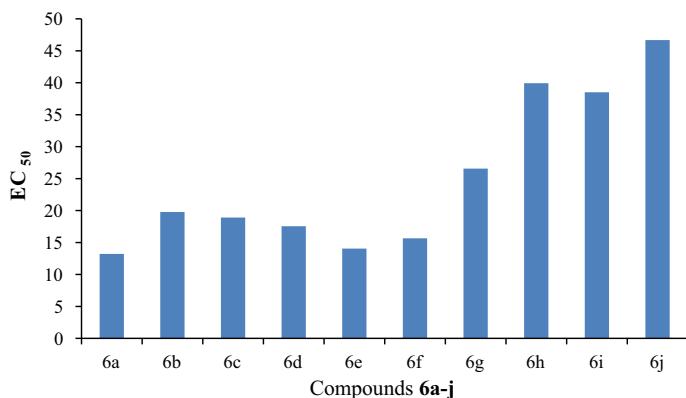


Fig. 3 EC₅₀ values of compounds **6a–j** on H₂O₂-induced PC12 cells

concentration. Furthermore, the *para* bromo-substituted derivative **6i** showed more protectivity than that of compound **6j** which is a *meta* bromo-substituted derivative at 40 and 50 $\mu\text{g/ml}$ concentrations. At 50 $\mu\text{g/ml}$ concentration, the cell viability of compound **6i** is $75.24 \pm 0.48\%$ where as for compound **6j** it is $66.21 \pm 0.46\%$. From these results, it can be understood that *ortho* and *para* positions are preferred for halogens to exhibit good neuroprotectivity.

Neurotoxicity of compounds in PC12 cell lines

One of the major hindrances in developing effective neuroprotective drugs is their toxicity to normal cells. In order to investigate the safety index of these potent neuroprotective agents, all the compounds were tested for cytotoxicity by using MTT assay in neuroblastoma cells (PC12). After incubating the cells with compounds for different times, the CC₅₀ values were calculated and are shown in Fig. 4. Among all the compounds, **6a**, **6e** and **6f** showed low toxicity with CC₅₀

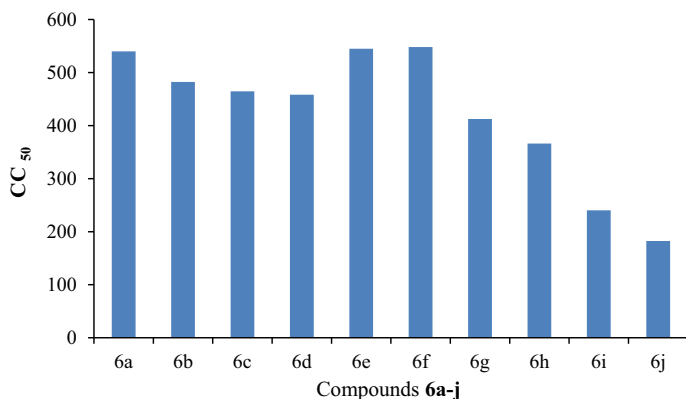


Fig. 4 Cytotoxicity of compounds **6a–j** on PC12 cells

values 540, 544.88 and 548.14 $\mu\text{g/ml}$, respectively. Compounds **6b**, **6c**, **6d** and **6g** showed moderate toxicity with CC_{50} values ranging from 412.36 to 482.26 $\mu\text{g/ml}$. The remaining compounds **6h**, **6i** and **6j** showed high toxicity.

Molecular docking studies

The docking protocol was validated using redocking experiments by removing the native ligand Ar-A014418 from GSK-3 β and docking back into the same binding pocket using Auto Dock 4.2 in PyRx with default parameters. It showed an RMSD value of 0.689 \AA , obtained from all atoms and heteroatom coordinates between experimental and redocked confirmations. Moreover, as shown in Fig. 5, the docked native ligand (blue-colored ligand in Fig. 5) is bound tightly to GSK-3 β involving almost the same residues Ile62, Ala83, Asp133, Tyr134, Val135, and Leu188 as in the co-crystallized structure (purple-colored ligand in Fig. 5). This indicates that

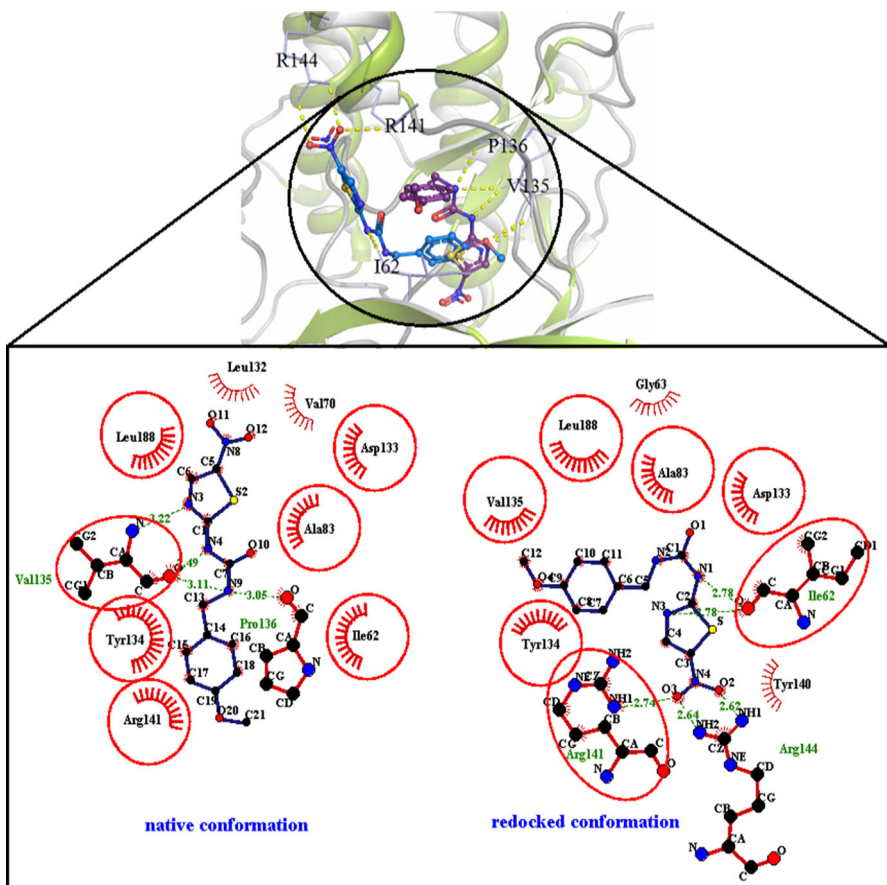


Fig. 5 Docking validation performed by re-docking native ligand into the ATP pocket of GSK-3 β . Docked pose is shown in blue and native conformation is shown in purple. (Color figure online)

these parameters are adequate in reproducing the experimental structure and can be extended to do docking studies on our synthesized compounds.

The molecular docking results revealed that all the compounds **6a–j** tend to bind within the ATP pocket of GSK-3 β and show good binding free energies ranging from -8.3 to -6.21 kcal/mol. The docking results are summarized in Table 2. Compound **6e** showed the highest binding energy of -8.3 kcal/mol and the lowest inhibition constant of 0.82 followed by compounds **6a** and **6f** which showed binding energies of -7.51 and -6.99 kcal/mol and inhibition constants of 3.13 and 7.53, respectively. The more negative value of binding energy and low inhibition constant indicate good binding affinity of the ligand towards the target enzyme. Thus, these results correlate well with the observed *in vitro* neuroprotective activity.

The 3D and 2D visualization of the interactions of the most active compounds **6e**, **6a** and **6f** within the ATP pocket of GSK-3 β are shown in Fig. 6. The binding models indicate that the compounds are held in the active site by a combination of various hydrogen bonding and hydrophobic interactions. Four hydrogen bonds were present in the derivative **6e**, which was the highest among the series. It showed hydrogen bonding interactions with amino acid residues Arg141, Arg144, Tyr134 and Val135 at the bond distances of 2.7, 3.0, 2.7 and 3.3 Å, respectively. The NH₂ group of Arg141 and Arg144 residues showed hydrogen bonding with oxygen of the nitro group on the phenyl ring (linked to the triazole) which is not seen in other molecules. This is evidence for the requirement of hydrophilic groups to bind strongly to the protein active site. The OH group of Tyr 134 and the NH group of Val 135 participated in hydrogen bonding with oxygen atoms of oxime and coumarin carbonyl oxygen, respectively. The coumarin moiety of **6e** occupies the hydrophobic pocket bounded by Leu188 and Val70 residues whereas the triazole ring is located in a pocket defined by the Ile62 residue. Furthermore, in compound **6a**, the coumarin moiety sits inside the hydrophobic pocket formed by Pro191, Glu137 and Pro136 residues while the phenyl ring (linked to triazole) is positioned in the pocket designed by Ile62 and Leu188 residues. In addition, it was also found to engage in three hydrogen bonding interactions with the OH group of the Tyr134 residue using oxygen and nitrogen atoms of oxime linkage and coumarin carbonyl oxygen at the distances of 2.6, 2.7 and 3.0 Å. Moreover, compound **6f** participated in hydrogen bonding with the NH₂ group of Arg141 residue using oxygen atoms of oxime and the coumarin carbonyl group at the distances of 3.1 and 3.3 Å. Regarding the hydrophobic interactions of compound **6f**, the coumarin moiety is engaged in the pocket formed by Gln185 and Ile62 residues, meanwhile the phenyl ring (linked to triazole) occupied the hydrophobic pocket formed by Tyr134, Leu188 and Ala83 residues. On the basis of activity and docking studies, it was found that compound **6e** had the improved potential to protect the PC12 cell lines against H₂O₂ oxidative stress.

In silico ADME prediction of compounds **6a–j**

Nowadays, many potential drugs fail to reach the clinic because of ADMET liabilities. Adsorption, distribution, metabolism, excretion and toxicity (ADMET) processes play a pivotal role in defining the therapeutic efficacy of a drug. Drug

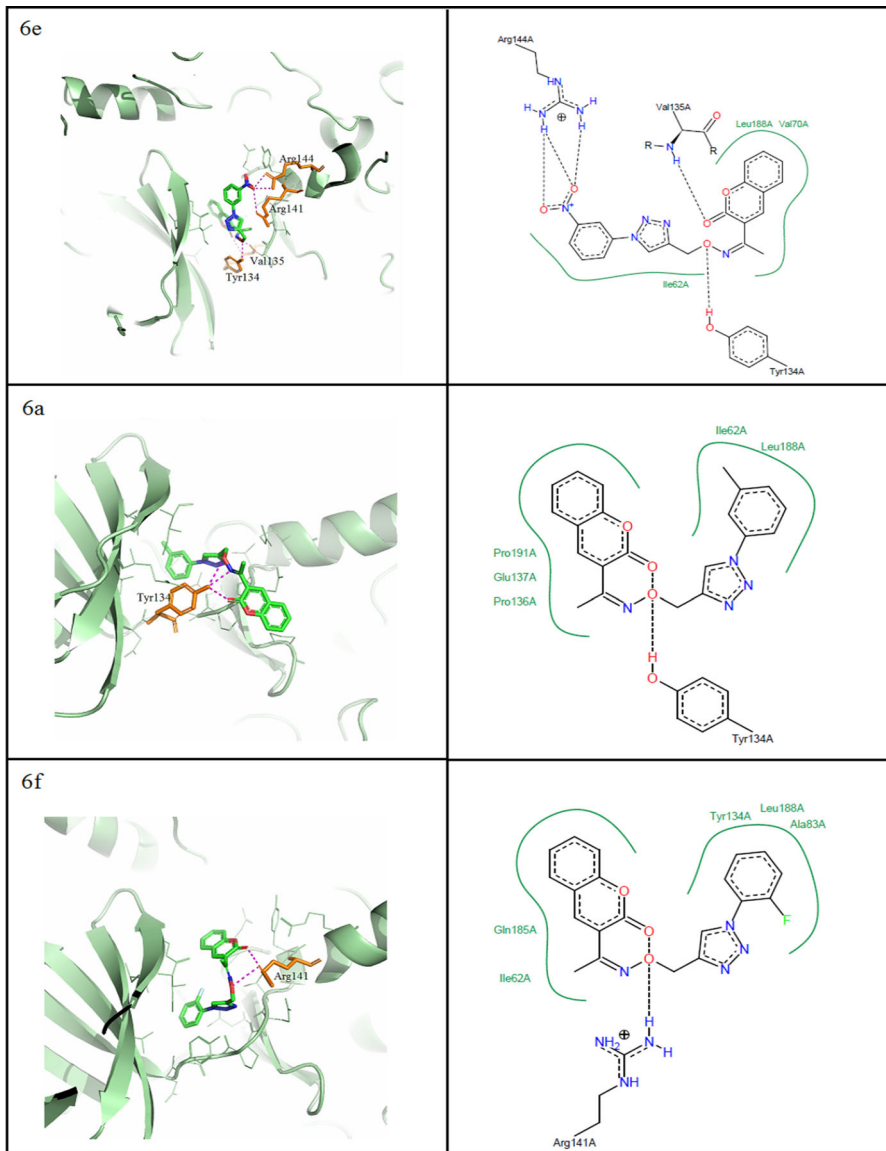


Fig. 6 Schematic diagram representing the 3D and 2D modeled binding modes of compounds **6e**, **6a** and **6f** within the ATP domain of GSK-3 β

likeness appears as a promising paradigm of a compound that optimizes their ADME in the human body [33].

With the aim of estimating the drug-likeness of the compounds, we have determined the compliance of the synthesized molecules to the Lipinski's 'rule of five'. According to this rule, poor absorption or permeation is more likely when there are more than five hydrogen bond donors, ten hydrogen bond acceptors, the

molecular weight is greater than 500 and the calculated $\log p$ (logarithmic ratio of the octanol–water partitioning coefficient) is greater than 5. Molecules violating more than one of these parameters may have problems with bioavailability and a high probability of failure to display drug-likeness [34]. Further, the topological polar surface area (TPSA) which is another key property in estimating drug bioavailability was also calculated. Generally, compounds with a TPSA $> 140 \text{ \AA}^2$ are thought to have low bioavailability [35]. As shown in Table 3, all the synthesized compounds comply with these rules. Moreover, all the compounds exhibited a greater percentage of absorption (%ABS) ranging from 64.7 to 80.5%. Hence, theoretically, all of these compounds should have good passive oral absorption and drug likeness.

In addition to this different ADME predictions, such as BBB penetration, percentage of human intestinal absorption (HIA%), CaCO_2 permeability and percentage of plasma protein binding (PPB%) were predicted for all compounds. Analyzing the ADME predictions (Table 4), it was observed that all the compounds showed high HIA% values in the range of 94.92–99.33% and are well absorbed. The CaCO_2 cell permeability values are moderate, ranging from 6.88 to 24.79 nm/s. Furthermore, all the compounds were strongly bound to plasma proteins with %PPB penetration more than 91.25%. In addition, they were found to have moderate

Table 3 Physicochemical properties of the compounds **6a–j**

Compound	Mol. wt ^a	Mol. vol ^b	<i>n</i> -ROTBC ^c	<i>n</i> -OHNH donor ^d	<i>n</i> -ON acceptor ^e	mi Log <i>P</i> ^f	TPSA (\AA^2) ^g	Lipinski's violation	%ABS ^h
Rule	≤ 500			≤ 5	≤ 10	≤ 5		≤ 1	
6a	374.4	330.3	5	0	7	3.65	82.53	0	80.5
6b	378.3	319.0	5	0	7	3.56	82.53	0	80.5
6c	390.4	339.6	6	0	8	3.26	91.76	0	77.3
6d	428.3	345.3	6	0	7	4.29	82.53	0	80.5
6e	405.3	337.4	6	0	10	3.35	128.35	0	64.7
6f	378.3	319.0	5	0	7	3.53	82.53	0	80.5
6g	360.3	314.0	5	0	7	3.21	82.53	0	80.5
6h	394.8	327.6	5	0	7	3.88	82.53	0	80.5
6i	439.2	331.9	5	0	7	4.01	82.53	0	80.5
6j	439.2	331.9	5	0	7	4.20	82.53	0	80.5

^aMolecular weight

^bMolecular volume

^cNumber of rotatable bonds

^dNumber of hydrogen bond donors

^eNumber of hydrogen bond acceptors

^fLogarithmic ratio of the octanol–water partitioning coefficient

^gTopological polar surface area

^hPercentage of absorption. %ABS = $109 - (0.345 \times \text{TPSA})$

Table 4 Prediction of pharmacokinetic properties of compounds **6a–j**

Compound	CaCO ₂ ^a permeability	HIA ^b (%)	PPB ^c (%)	BBB ^d (C _{brain} /C _{blood})
6a	23.43	98.81	92.27	0.117
6b	24.79	98.93	92.73	0.479
6c	20.74	99.33	91.25	0.355
6d	20.93	98.78	92.87	0.443
6e	6.88	94.92	93.60	0.193
6f	23.39	98.93	92.14	0.374
6g	20.84	98.93	92.79	0.319
6h	21.82	98.22	95.95	0.345
6i	21.99	97.78	100.00	0.325
6j	22.14	97.78	94.88	0.548

^aColon adenocarcinoma^bHuman intestinal absorption^cPlasma protein binding^dBlood–brain barrier

penetration (0.117–0.548) to the CNS through the BBB. From all these parameters, it can be observed that, theoretically, all the compounds exhibited good absorption and bioavailability with reasonable permeability through the BBB.

Conclusion

With the aim of synthesizing more potent neuroprotective agents, we focused our attention on the synthesis of coumarin and 1,2,3-triazole linked moieties **6a–j** by copper(1)-catalyzed 1,3-dipolar azide–alkyne cycloaddition (CuAAC) reaction to achieve quantitative yields, and examined their neuroprotective activity against H₂O₂-induced PC12 neurons and toxicity using MTT reduction assay. Of all the compounds, **6a**, **6e** and **6f** showed better neuroprotective activity with EC₅₀ values 13.21, 14.04 and 15.66 µg/ml, respectively. Compounds **6f**, **6e** and **6a** showed low toxicity with CC₅₀ values 548.14, 544.88 and 540 µg/ml, respectively. In addition to that compound, **6e** showed the highest cell viability (94.51 ± 0.68%) against H₂O₂-induced PC12 cell lines at 50 µg/ml concentration. From these results, it can be concluded that compound **6e** was a better neuroprotective agent with low toxicity. Further molecular docking studies between the synthesized molecules **6a–j** and GSK-3β enzyme ATP binding pocket revealed that compound **6e** showed higher binding affinities and many more interactions when compared to other compounds. In addition, in silico ADME prediction showed that all the compounds fulfilled Lipinski's rule of five with moderate potential to penetrate the BBB. These results suggested that compound **6e** can be considered as a promising candidate for further optimization and development of potential neuroprotective drugs.

Acknowledgements One of the authors (MAK) gratefully acknowledges UGC for providing financial assistance in the form of a BSR fellowship. Funding was provided by University Grants Commission (Grant No. F.25-1/2013-14 (BSR)/7-187/2007 (BSR)).

References

1. G.C. Gonzalez-Munoz, M.P. Arce, M.G. Lopez, B. Lopez, C. Perez, M. Villarroya, M.G. Lopez, A.G. Garcia, S. Conde, M.I.R. Franco, *Eur. J. Med. Chem.* **45**, 6152 (2010)
2. D. Pratico, *Trends Pharmacol. Sci.* **29**, 609 (2008)
3. K.J. Barnham, C.L. Masters, A.I. Bush, *Nat. Rev. Drug Discov.* **3**, 205 (2004)
4. S.F. Wang, Y. Yin, X. Wu, F. Qiao, S. Sha, P.C. Lv, J. Zhao, H.L. Zhu, *Bioorg. Med. Chem.* **22**, 5727 (2014)
5. Q. Ji, Z. Ge, Z. Ge, K. Chen, H. Wu, X. Liu, Y. Huang, L. Yuan, X. Yang, F. Liao, *Eur. J. Med. Chem.* **108**, 166 (2016)
6. W. Zhang, Z. Li, M. Zhou, F. Wu, X. Hou, H. Luo, H. Liu, X. Han, G. Yan, Z. Ding, R. Li, *Bioorg. Med. Chem. Lett.* **24**, 799 (2014)
7. M.Z. Hassan, H. Osman, M.A. Ali, M.J. Ahsan, *Eur. J. Med. Chem.* **123**, 236 (2016)
8. T.O. Olomola, R. Klein, N. Mautsa, Y. Sayed, P.T. Kaye, *Bioorg. Med. Chem.* **21**, 1964 (2013)
9. L. Lei, Y.B. Xue, Z. Liu, S.S. Peng, Y. He, Y. Zhang, R. Fang, J.P. Wang, Z.W. Luo, G.M. Yao, J.W. Zhang, G. Zhang, H.P. Song, Y.H. Zhang, *Sci. Rep.* **5**, 13544 (2015)
10. M. Khoobi, S. Emami, G. Dehghan, A. Foroumadi, A. Ramazani, A. Shafiee, *Arch. Pharm. Chem. Life Sci.* **344**, 588 (2011)
11. E. Grimm, C. Brideau, N. Chauret, C. Chan, D. Delorme, Y. Ducharme, D. Ethier, J. Falguyet, R. Friesen, J. Guay, P. Hamel, D. Riendeau, C.S. Breau, P. Tagari, Y. Girard, *Bioorg. Med. Chem. Lett.* **16**, 2528 (2006)
12. D.H. Dawood, R.Z. Batran, T.A. Farghaly, M.A. Khedr, M.M. Abdulla, *Arch. Pharm. Chem. Life Sci.* **348**, 875 (2015)
13. S. Manfredini, C.B. Vicentini, M. Manfrini, N. Bianchi, C. Rutigliano, C. Mischiati, R. Gambari, *Bioorg. Med. Chem.* **8**, 2343 (2000)
14. K. Lal, P. Yadav, A. Kumar, *Med. Chem. Res.* **25**, 644 (2016)
15. É. Bokor, T. Docsa, P. Gergely, L. Somsák, *Bioorg. Med. Chem.* **18**, 1171 (2010)
16. T.W. Kim, Y. Yong, S.Y. Shin, H. Jung, K.H. Park, Y.H. Lee, Y. Lim, K.Y. Jung, *Bioorg. Chem.* **59**, 1 (2015)
17. J.L. Kelley, C.S. Koble, R.G. Davis, E.W. McLean, F.E. Soroko, B.R. Coopert, *J. Med. Chem.* **38**, 4131 (1996)
18. P. Passannanti, P. Diana, F. Barraja, A. Mingoia, G. Lauria, *Cirriuncione. Heterocycles* **48**, 1229 (1998)
19. N. Devender, S. Gunjan, S. Chhabra, K. Singh, V.R. Pasam, S.K. Shukla, A. Sharma, S. Jaiswal, S.K. Singh, Y. Kumar, J. Lal, A.K. Trivedi, R. Tripathi, R.P. Tripathi, *Eur. J. Med. Chem.* **109**, 187 (2016)
20. A.K. Jordao, P.P. Afonso, V.F. Ferreira, M.C.B.V. de Souza, M.C.B. Almeida, C.O. Beltrame, D.P. Paiva, S.M.S.V. Wardell, J.L. Wardell, E.R.T. Tiekink, C.R. Damaso, A.C. Cunha, *Eur. J. Med. Chem.* **44**, 3777 (2009)
21. M. Sun, J. Hu, X. Song, D. Wu, L. Kong, Y. Sun, D. Wang, Y. Wang, N. Chen, G. Lui, *Eur. J. Med. Chem.* **67**, 39 (2013)
22. A. Asadipour, M. Alipour, M. Jafari, M. Khoobi, S. Emami, H. Nadri, A. Sakhteman, A. Moradi, V. Sheibani, F.H. Moghadam, A. Shafiee, A. Foroumadi, *Eur. J. Med. Chem.* **70**, 623 (2013)
23. C. Hooper, R. Killick, S. Lovestone, *J. Neurochem.* **104**(6), 1433 (2008)
24. Mudasir Maqbool, Mohammad Mobashir, Nasimul Hoda, *Eur. J. Med. Chem.* **107**, 63 (2016)
25. G.M. Morris, R. Huey, W. Lindstrom, M.F. Sanner, R.K. Belew, D.S. Goodsell, A.J. Olson, *J. Comput. Chem.* **30**, 2785 (2009)
26. E. ter Haar, J.T. Coll, D.A. Austen, H.M. Hsiao, L. Swenson, J. Jain, *Nat. Struct. Biol.* **8**, 593 (2001)
27. E.F. Pettersen, T.D. Goddard, C.C. Huang et al., *J. Comput. Chem.* **25**, 1605 (2004)
28. Y. Zhao, M.H. Abraham, J. Lee, A. Hersey, N.C. Luscombe, G. Beek, B. Sherborne, I. Cooper, *Pharm. Res.* **19**, 1446 (2002)
29. G. Walkinshaw, C.M. Waters, *Neuro Science* **63**, 975 (1994)

30. I.Z. Tao, X.F. Li, I.I. Zhang, J.Y. Tian, X.B. Li, X. Sun, X.F. Li, I. Jiang, X.J. Zhang, J.Z. Chen, *PLoS ONE* **6**, 1 (2011)
31. H. Garn, H. Krause, V. Enzmann, K. Drassler, *Immunol. Method* **168**, 253 (1994)
32. S.M. Thom, R.W. Horobin, E. Seidler, M.R. Barer, *Appl. Bacteriol.* **74**, 433 (1993)
33. G. Vistoli, A. Pedretti, B. Testa, *Drug Discov. Today* **13**(7–8), 285 (2008)
34. C.A. Lipinski, F. Lombardo, B.W. Dominy, P.J. Feeny, *Adv. Drug Deliv. Rev.* **23**, 3 (1997)
35. D.E. Clark, S.D. Pickett, *Drug Discov. Today* **5**, 49 (2000)